

Cascaded H-bridge Converter-Based Flexible Arc Suppression Method Adapting to Line Parameter Variations

Guojun Zhao, Moufa Guo, *Member, IEEE*, Binlong Zhang, *Student Member, IEEE*, Zeyin Zheng, *Member, IEEE*, and Qiteng Hong, *Senior Member, IEEE*

Abstract—Single-phase grounding faults in distribution networks can generate arcs, posing significant risks such as electric shock and forest fires. The flexible arc suppression device is capable of suppressing the arc. However, traditional flexible arc suppression devices do not account for line voltage drop and asymmetry in ground parameters when calculating the injection current reference value. Consequently, changes in ground fault conditions can impair the effectiveness of zero residual current suppression, undermining the reliability of arc suppression. To address this issue, this paper proposes a flexible arc suppression method that adapts to line parameter variations. This paper provides a theoretical analysis of the differences between the newly deduced arc suppression algorithm and the original algorithm, with a focus on zero-sequence voltage regulation and ground fault current suppression. The analysis elucidates the law of parameter variations governing the dominant zero-sequence voltage difference after regulation. Subsequently, an adaptive injection current arc suppression algorithm is proposed based on this law, which accommodates changes in line parameters. Compared to traditional methods, the proposed algorithm demonstrates enhanced adaptability to variations in grounding fault parameters and significantly improves current suppression effectiveness. The correctness and feasibility of the method are validated through PSCAD/EMTDC simulations and physical experiments.

Index Terms—distribution network, sing-phase grounding fault, flexible arc suppression method, power electronic technology, cascaded H-bridge flexible arc suppression device.

This work was supported in part by the Natural Science Foundation of Fujian Province, China, under Award 2023J05106. (Corresponding authors: Moufa Guo).

Guojun Zhao, Moufa Guo, and Zeyin Zheng are with the College of Electrical Engineering and Automation, Fuzhou University, Fuzhou 350108, China, and also with the Engineering Research Center of Smart Distribution Grid Equipment, Fujian Province University, Fuzhou 350108, China (e-mail: 230110013@fzu.edu.cn; gmf@fzu.edu.cn; zhengzeyin@fzu.edu.cn).

Binlong Zhang is with the College of Electrical Engineering and Automation, Fuzhou University, Fuzhou 350108, China, and also with the Department of Electrical Engineering, Yuan Ze University, Taoyuan 32003, Taiwan (e-mail: 220110011@fzu.edu.cn).

Qiteng Hong is with the Department of Electronic and Electrical Engineering, University of Strathclyde, G1 1RD Glasgow, U.K. (e-mail: q.hong@strath.ac.uk).

Color versions of one or more of the figures in this article are available online at <http://ieeexplore.ieee.org>

I. INTRODUCTION

THE distribution network comprises numerous branches, operates in dynamic environments, and is prone to faults [1]. Additionally, over 80% of these faults are single-phase ground faults [2]. The arc generated by single-phase ground faults can lead to overvoltages, posing significant risks to power equipment and potentially causing hazards such as electric shocks and forest fires [3], [4]. Therefore, the effective suppression of fault-induced arcs is essential for improving system safety and reliability.

The effectiveness of AC arc extinguishing is governed by the interplay between the recovery rate of dielectric insulation strength and the rate of voltage reestablishment [5]. After the arc current crosses zero, the grounding arc can be extinguished without reignition if the recovery rate of dielectric strength at the fault point exceeds the voltage recovery rate [6]. Based on ground fault suppression principles, arc suppression coils have been widely used in distribution networks [7], [8]. With the increase of cable lines and the widespread use of nonlinear loads, the proportion of active and harmonic components in ground fault currents has significantly increased [9]. Under these conditions, the arc suppression coil, due to its inherent characteristics, compensates only for the fundamental component of the current and is ineffective against the active and harmonic components. In certain operational scenarios, the residual current following arc suppression coil compensation remains sufficient to sustain arc ignition [10]. The grounding fault transfer arc suppression device proposed in [11] is unaffected by current components. This device directly grounds the fault-phase bus via a circuit breaker, achieving arc suppression. However, this approach is unable to adapt to variations in transition resistance at the fault point, and in the case of a metallic grounding fault, the fault current cannot be bypassed. The above arc suppression method is passive, unable to adapt to changes in ground fault conditions, and has limitations.

Power electronics technology, characterized by its controllability of both voltage and current, has therefore prompted researchers to propose an inverter-based flexible arc suppression method [2], [12]. The core principle of this method involves injecting a controllable current into the neutral point or bus of the distribution network via an inverter to suppress both the voltage and current at the fault point.

Based on control target values, flexible arc suppression methods are categorized into voltage-type and current-type approaches. The voltage-type flexible arc suppression method directly controls the fault phase voltage at the bus to zero or adjusts the neutral point voltage to the negative value of the fault phase supply voltage, indirectly reducing the fault phase voltage to zero [13]. Thus, the control target for this method can either be zero or the negative value of the fault phase supply voltage [14], [15]. The current-type flexible arc suppression method calculates the compensation current by multiplying the negative value of the fault phase supply voltage by the ground admittance of the distribution network [16], [17]. This compensation current is injected into the system's neutral point, making the neutral point voltage negative relative to the fault phase supply voltage. Consequently, this method indirectly suppresses both the fault phase voltage and the fault point current.

In practical applications, line impedance introduces a voltage drop, causing the fault phase voltage at the bus to deviate from the fault point voltage. The influence of line voltage drop is neglected in the calculation of the control target value in the voltage-type flexible arc suppression method [18]. In the case of small transition resistance grounding faults near the end of long, heavily loaded lines, the voltage-type flexible arc suppression method may not only increase the fault point current but also exacerbate the severity of the arc [19]. In contrast, the current-type flexible arc suppression method is lightly affected by line voltage drops. As a result, the current-type flexible arc suppression method has garnered attention from scholars worldwide [20], [21], [22], [23]. To improve the grounding fault suppression performance, references [17], [24], [25] have conducted in-depth research on the measurement of ground parameters and made significant progress in both theoretical and field applications. Moreover, researchers have conducted in-depth studies on control and modulation strategies [26], [27], [28], establishing a solid foundation for achieving the control objectives of the flexible arc suppression method. However, the calculation of the given value of the control target ignores the influence of the fault line voltage drop in the current-type flexible arc suppression method. At this time, there is a theoretical error in the calculation of the given value of the current-type flexible arc suppression method. The residual current caused by the theoretical error always exists. No matter how the control strategy is improved, the arc suppression performance of the flexible current arc suppression method cannot be further improved.

In summary, the control target value for the current-type flexible arc suppression method is defined as the product of the negative fault phase source voltage and the ground admittance. However, the calculation of this control target value neglects the impact of fault line voltage drop. While the current-type method is less affected by voltage drop than the voltage-type method, the specific extent of this influence remains underexplored. Moreover, the existing literature lacks a theoretical framework to explain the conditions under which

the impact of voltage drop can be disregarded. This represents a major obstacle to further enhancing the arc suppression performance of current-type flexible arc suppression methods. Therefore, it is essential to evaluate the adaptability of this method to variations in single-phase grounding fault conditions. Such an assessment will provide the necessary theoretical foundation for achieving zero residual current suppression in the flexible arc suppression systems of distribution networks, ensuring reliable arc suppression.

In light of the aforementioned challenges, this paper presents an in-depth analysis of the reasons why the traditional current-type flexible arc suppression method fails to achieve zero residual current, particularly due to line voltage drops and asymmetry in three-phase ground parameters. A novel injection current formula is derived to achieve zero residual current suppression for ground faults. However, this formula requires the parameter value of the line voltage drop. To address this, a flexible arc suppression method that adapts to variations in line parameters is proposed. This approach eliminates the need for voltage drop measurements in the fault feeder and achieves zero residual current suppression under varying single-phase grounding fault conditions.

The remainder of this paper is organized as follows: Section II examines the effects of line voltage drop and asymmetry in three-phase-to-ground parameters on the performance of the current-type flexible arc suppression method. Section III introduces a flexible arc suppression method incorporating adaptive line parameters. Section IV validates this method through software simulations and physical experiments. Finally, Section V presents the conclusions.

II. PRINCIPLE OF FLEXIBLE ARC SUPPRESSION METHOD

A. Current-Type Flexible Arc Suppression Method with Neglect of Line Voltage Drop

The arc suppression diagram of the cascaded H-bridge flexible arc suppression device (FASD) connected to the neutral point of the distribution network is shown in Fig. 1.

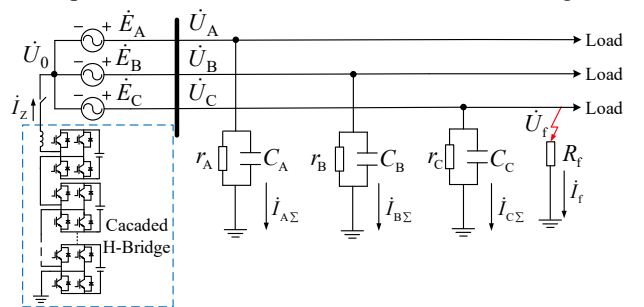


Fig. 1. Single-phase ground fault arc suppression diagram for a distribution network.

In Fig. 1, \dot{E}_A , \dot{E}_B , and \dot{E}_C represent the phase voltages of the distribution network; \dot{U}_A , \dot{U}_B , and \dot{U}_C denote the bus voltages of each phase; \dot{U}_0 is the neutral point voltage; \dot{U}_f is the fault point voltage; I_f is the fault point current; r_A , r_B , and r_C represent the phase-to-ground leakage resistances; C_A , C_B , and C_C are the phase-to-ground capacitances; R_f is the

transition resistance; \dot{I}_z is the output current of the cascaded H-bridge FASD.

As shown in Fig. 1, the fault point current can be expressed as

$$\dot{I}_f = \frac{\dot{E}_C + \dot{U}_0}{R_f} = \frac{\dot{U}_f}{R_f} \quad (1)$$

If $\dot{U}_0 = -\dot{E}_C$, then $\dot{U}_f = 0$, and $\dot{I}_f = 0$. The arc-suppression principle is consistent with the approach presented in [6], [10], [12], [14], and [15].

According to Kirchhoff's law and as shown in Fig. 1, the expression for the injection current of the FASD is given by (2).

$$(\dot{E}_A + \dot{U}_0)Y_A + (\dot{E}_B + \dot{U}_0)Y_B + (\dot{E}_C + \dot{U}_0)Y_C + \frac{\dot{E}_C + \dot{U}_0}{R_f} = \dot{I}_z \quad (2)$$

In (2), Y_A , Y_B , and Y_C denote the ground admittances of the three-phase distribution network, respectively.

When the three-phase power supply and the ground parameters of the distribution network are symmetrical, (2) can be expressed as

$$\dot{U}_0 Y_0 + \frac{\dot{E}_C + \dot{U}_0}{R_f} = \dot{I}_z \quad (3)$$

In (3), $Y_0 = 3Y_A = 3Y_B = 3Y_C = 1/Z_0$.

Given the condition $\dot{U}_0 = -\dot{E}_C$, the calculation formula for the injection current of the FASD can be derived as follows

$$\dot{I}_z = -\dot{E}_C \frac{1}{Z_0} \quad (4)$$

The injected current formula applied in [5], [9], [20], [23], and [26] corresponds to the one provided in (4).

Eq. (4) is derived under the assumption of symmetrical three-phase-to-ground parameters. When the three-phase ground parameters are asymmetric, the calculation formula for the injection current of the FASD is

$$\dot{I}_{zz} = -\dot{E}_C Y_{\Sigma ABC} - (\dot{E}_A Y_A + \dot{E}_B Y_B + \dot{E}_C Y_C) \quad (5)$$

In (5), $Y_{\Sigma ABC} = Y_A + Y_B + Y_C = 1/Z_{\Sigma ABC}$. Y_A , Y_B , and Y_C , need to be measured individually. To avoid the need for measuring Y_A , Y_B , and Y_C , the neutral point displacement voltage \dot{U}_{00} under normal operating conditions of the distribution network can be used to replace $\dot{E}_A Y_A + \dot{E}_B Y_B + \dot{E}_C Y_C$ in (5). Under normal operating conditions of the distribution network, the neutral point displacement voltage, as shown in Fig. 1, can be expressed as

$$\dot{U}_{00} = -\frac{\dot{E}_A (Y_A + a^2 Y_B + a Y_C)}{Y_A + Y_B + Y_C} \quad (6)$$

In (6), $a = 1 \angle 120^\circ$. The expression for the injected current, after substituting (6) into (5) and performing parameter replacement, is obtained as follows

$$\dot{I}_{zz} = -(\dot{E}_C + \dot{U}_{00}) \frac{1}{Z_{\Sigma ABC}} \quad (7)$$

Compared to (5), (7) eliminates the need to measure each relative ground parameter individually, requiring only the measurement of the overall ground parameters of the distribution network.

B. Current-Type Flexible Arc Suppression Method Accounting for Line Voltage Drop

As shown in Fig. 1, when considering the line voltage drop \dot{U}_{zL} , the expression for the fault point current in the distribution network is given by

$$\dot{I}_f = \frac{\dot{U}_f}{R_f} = \frac{\dot{E}_C + \dot{U}_0 - \dot{U}_{zL}}{R_f} \quad (8)$$

If $\dot{U}_0 = -\dot{E}_C + \dot{U}_{zL}$, then $\dot{U}_f = 0$, and $\dot{I}_f = 0$. According to Kirchhoff's law, the expression for the injection current of the FASD can be obtained as follows

$$(\dot{E}_A + \dot{U}_0)Y_A + (\dot{E}_B + \dot{U}_0)Y_B + (\dot{E}_C + \dot{U}_0)Y_C + \frac{\dot{E}_C + \dot{U}_0 - \dot{U}_{zL}}{R_f} = \dot{I}_{zL} \quad (9)$$

When the three-phase power supply and the three-phase ground parameters of the distribution network are symmetrical, (9) can be expressed as follows

$$\dot{U}_0 Y_0 + \frac{\dot{E}_C + \dot{U}_0 - \dot{U}_{zL}}{R_f} = \dot{I}_{zL} \quad (10)$$

Given the condition $\dot{U}_0 = -\dot{E}_C + \dot{U}_{zL}$, the calculation formula for the injection current of the FASD can be derived from (10) as follows

$$\dot{I}_{zL} = (-\dot{E}_C + \dot{U}_{zL}) \frac{1}{Z_0} \quad (11)$$

When the three-phase-to-ground parameters are asymmetric, the calculation formula for the injection current can be expressed as follows

$$\dot{I}_{z0L} = -(\dot{E}_C - \dot{U}_{zL} + \dot{U}_{00}) \frac{1}{Z_{\Sigma ABC}} \quad (12)$$

Compared to (7), (12) incorporates the compensation term for \dot{U}_{zL} . When accounting for the line voltage drop and the asymmetry of the three-phase ground parameters, the FASD theoretically achieves $\dot{U}_f = 0$, and $\dot{I}_f = 0$. when using (12) as the specified value for the current control target.

In (12), \dot{U}_{00} can be measured before a distribution network fault occurs, whereas \dot{U}_{zL} must be measured after a ground fault. Since \dot{U}_{zL} is influenced by load current and line impedance, and given the complex structure of distribution networks, obtaining accurate parameters for load current and line impedance is often challenging. As a result, practical engineering frequently neglects the impact of \dot{U}_{zL} when calculating the reference value for the injection current of the FASD. Consequently, the arc suppression performance of the current-type flexible arc suppression method, which disregards \dot{U}_{zL} , will be analyzed in the following section.

C. Analysis of Ground Fault Suppression Performance of Current-Type Flexible Arc Suppression Method

When the three-phase power supply and the three-phase ground parameters of the distribution network are symmetrical, the FASD uses (4) as the target value for current control. After the current is injected, the zero-sequence voltage of the distribution network can be expressed as

$$\dot{U}_{01} = -\dot{E}_C + \dot{U}_{zL} \frac{1}{1 + R_f/Z_0} \quad (13)$$

From (13), it can be observed that, in the presence of \dot{U}_{zL} , regulating \dot{U}_{01} to $-\dot{E}_C$ is conditional. Specifically,

when $|R_f| \gg |Z_0|$, $\dot{U}_{01} \approx -\dot{E}_C$. Conversely, when $|R_f| \ll |Z_0|$, $\dot{U}_{01} \approx -\dot{E}_C + \dot{U}_{ZL}$.

It can be observed that \dot{U}_{01} can be easily regulated to $-\dot{E}_C$ in the case of high resistance, resulting in $I_f \approx 0$. However, in the case of low resistance, \dot{U}_{ZL} will induce a residual current at the fault point. The expression for the residual current at the fault point is

$$\dot{I}_{f1_UL} = \frac{\dot{U}_{ZL}}{Z_0 + R_f} \quad (14)$$

From (14), it is evident that when \dot{U}_{ZL} is fixed, \dot{I}_{f1_UL} is influenced by Z_0 and R_f . Z_0 is primarily related to the ground capacitance C_0 of the distribution network; specifically, a larger C_0 results in a smaller Z_0 . Consequently, when \dot{U}_{ZL} remains constant, an increase in C_0 leads to a decrease in R_f , thereby causing \dot{I}_{f1_UL} to increase.

When the three-phase ground parameters are asymmetric, the FASD uses (4) as the target value for current control. After the current is injected, the zero-sequence voltage of the distribution network can be expressed as

$$\dot{U}_{02} = -\dot{E}_C + \dot{U}_{ZL} \left(\frac{1}{1 + R_f/Z_{\Sigma ABC}} \right) + \dot{U}_{00} \left(\frac{1}{1 + Z_{\Sigma ABC}/R_f} \right) \quad (15)$$

At this point, the expression for the residual current at the fault point is given by

$$\begin{aligned} \dot{I}_{f2} &= \frac{\dot{U}_{ZL}}{Z_{\Sigma ABC} + R_f} - \frac{\dot{U}_{00}}{R_f + Z_{\Sigma ABC}} \\ &= \dot{I}_{f2_UL} - \dot{I}_{f2_U00} \end{aligned} \quad (16)$$

Compared to (14), (16) includes the residual current \dot{I}_{f2_U00} caused by \dot{U}_{00} .

It can be observed that when the three-phase ground parameters of the distribution network are asymmetric, injecting current according to (4) with the FASD results in a residual current \dot{I}_{f2} . \dot{I}_{f2} consists of \dot{I}_{f2_UL} and \dot{I}_{f2_U00} :

To eliminate the influence of the residual current \dot{I}_{f2_U00} , the FASD uses (7) as the target value for current control. After the current is injected, the zero-sequence voltage of the distribution network can be expressed as

$$\dot{U}_{03} = -\dot{E}_C + \dot{U}_{ZL} \left(\frac{1}{1 + R_f/Z_{\Sigma ABC}} \right) \quad (17)$$

From (17), it can be seen that after the FASD injects current according to (7), the zero-sequence voltage is less affected by \dot{U}_{00} compared to the scenario described in (15). Consequently, the fault point residual current is solely influenced by \dot{U}_{ZL} , as shown in (18).

$$\dot{I}_{f3} = \frac{\dot{U}_{ZL}}{Z_{\Sigma ABC} + R_f} = \dot{I}_{f2_UL} \quad (18)$$

Neither (4) nor (7) can eliminate the influence of the ground fault residual current caused by \dot{U}_{ZL} .

When the three-phase power supply of the distribution network is symmetrical, and the three-phase ground parameters are balanced, the FASD uses (11) as the reference value for the current control target. After the current is injected, the zero-sequence voltage of the distribution network can be expressed as

$$\dot{U}_{04} = -\dot{E}_C + \dot{U}_{ZL} \quad (19)$$

Therefore, $\dot{U}_f = 0$, and $\dot{I}_f = 0$.

When the three-phase ground parameters are asymmetric, the FASD uses (11) as the reference value for the current control target. After the current is injected, the zero-sequence voltage of the distribution network can be expressed as

$$\dot{U}_{05} = -\dot{E}_C + \dot{U}_{ZL} + \frac{\dot{U}_{00}}{1 + Z_{\Sigma ABC}/R_f} \quad (20)$$

Eq. (11) for the current control target accounts for the influence of line voltage drop but does not consider the effect of displacement voltage \dot{U}_{00} . Consequently, the residual current caused by displacement voltage \dot{U}_{00} is expressed in (21).

$$\dot{I}_{f5} = -\frac{\dot{U}_{00}}{R_f + Z_{\Sigma ABC}} \quad (21)$$

To eliminate the residual current, the FASD uses (12) as the reference value for the current control target. After the current is injected, the zero-sequence voltage of the distribution network can be expressed as

$$\dot{U}_{06} = -\dot{E}_C + \dot{U}_{ZL} \quad (22)$$

Eq. (22) shows that, after accounting for the line voltage drop and the asymmetry of the three-phase ground parameters, the zero-sequence voltage following current injection is identical to that given in (19). This effectively eliminates both the influence of displacement voltage caused by the asymmetry of the three-phase ground parameters and the effect of residual current. Therefore, $\dot{U}_f = 0$, and $\dot{I}_f = 0$.

In summary, the arc suppression effectiveness of the FASD, when using (12) as the reference value for the current control target, is superior to that achieved with (4), (7), and (11). This approach ensures that $\dot{U}_f = 0$ and $\dot{I}_f = 0$.

The \dot{U}_{ZL} in (12) is difficult to measure directly but can be calculated based on fault distance, line impedance, and load current. Unlike transmission networks, distribution networks have shorter lines, numerous branches, and a complex, variable operating environment. Measuring the fault distance in such conditions is challenging, complicating the acquisition of line voltage drop. Additionally, obtaining accurate load current and line impedance data is also complex. To address the issue of determining line voltage drop, this paper proposes a flexible arc suppression method with adaptive line parameters, aiming to achieve zero residual current in ground faults and enhance the reliability of arc suppression in such faults.

III. FLEXIBLE ARC SUPPRESSION METHOD OF ADAPTIVE LINE PARAMETER VARIATIONS

Based on the relationship between $|R_f|$ and $|Z_{\Sigma ABC}|$ in (17), the following relationship can be derived

$$\begin{cases} |R_f| \gg |Z_{\Sigma ABC}|, \dot{U}_{03} \approx -\dot{E}_X \\ |R_f| = |Z_{\Sigma ABC}|, \dot{U}_{03} = -\dot{E}_X + \frac{1}{2}\dot{U}_{ZL} \\ |R_f| \ll |Z_{\Sigma ABC}|, \dot{U}_{03} \approx -\dot{E}_X + \dot{U}_{ZL} \end{cases} \quad (23)$$

In (23), \dot{E}_X represents the phase power supply voltage. By comparing (22) and (23), it is observed that when $|R_f| \gg |Z_{\Sigma ABC}|$ in (23), $\dot{U}_{03} \approx -\dot{E}_X$. The influence of the line voltage drop \dot{U}_{ZL} can be ignored, resulting in $\dot{U}_f \approx 0$, $\dot{I}_f \approx 0$. Conversely, when $|R_f| \ll |Z_{\Sigma ABC}|$ in (23), $\dot{U}_{03} \approx -\dot{E}_X + \dot{U}_{ZL}$. Substituting the zero-sequence voltage \dot{U}_{03} under this condition into the numerator of (7), a new injection current calculation formula can be derived as follows

$$\dot{I}_{Z_new} = \frac{\dot{U}_{03}}{Z_0} \quad (24)$$

Eq. (24) incorporates the component of \dot{U}_{ZL} . Using it as a reference for the current control target in the FASD can eliminate residual current caused by \dot{U}_{ZL} .

Additionally, under the condition $|R_f| = |Z_{\Sigma ABC}|$, where $\dot{U}_{03} = -\dot{E}_X + (1/2)\dot{U}_{ZL}$, the zero-sequence voltage tends to shift toward either $\dot{U}_{03} \approx -\dot{E}_X$ or $\dot{U}_{03} \approx -\dot{E}_X + \dot{U}_{ZL}$, regardless of the variation in $|R_f|$. Therefore, when (24) is used as the reference value for the current control target of the FASD, the suppression of residual current caused by the line voltage drop can be achieved.

Based on the variation characteristics of zero-sequence voltage in (22) and (23), and the relationship between zero-sequence voltage and transition resistance after current injection, an injection current algorithm with adaptive line parameter variation can be designed to achieve the same arc suppression effect as in (12).

The injection current algorithm for adaptive line parameter variations is presented in (25).

In (25), \dot{I}_{Z_ref1} and \dot{I}_{Z_ref2} represent the given values of the current control target for the FASD at different time periods. \dot{I}_{Z_ref1} accounts for the influence of the displacement voltage \dot{U}_{00} , while \dot{U}_{Z_ref1} is the zero-sequence voltage after the FASD injects current based on the control target value \dot{I}_{Z_ref1} .

$$\begin{cases} \dot{I}_{Z_ref1} = -(\dot{E}_X + \dot{U}_{00}) \frac{1}{Z_{\Sigma ABC}} \\ \dot{I}_{Z_ref2} = \dot{U}_{Z_ref1} \frac{1}{Z_{\Sigma ABC}} \end{cases} \quad (25)$$

After a single-phase grounding fault occurs in the distribution network, \dot{I}_{Z_ref1} , as the initial current control target of the FASD, can eliminate the residual current caused by the displacement voltage \dot{U}_{00} . At this point, only the voltage drop residual current \dot{I}_{fl_UL} remains. In cases of high resistance, the influence of the line voltage drop \dot{U}_{ZL} can be neglected, resulting in $\dot{U}_f \approx 0$ and $\dot{I}_f \approx 0$. Additionally, when the line voltage drop \dot{U}_{ZL} is significant and the transition resistance is low, the current and voltage at the fault point will exhibit a downward trend. In this case, \dot{I}_{Z_ref2} is calculated based on the zero-sequence voltage \dot{U}_{Z_ref1} obtained after the injection of \dot{I}_{Z_ref1} , and is used as the second current control target of the FASD. This ensures that $\dot{U}_f \approx 0$ and $\dot{I}_f \approx 0$, regardless of the transition resistance.

Compared to (12), the injection current algorithm in (25) eliminates the need for load current, fault location, and line impedance calculations. The proposed method adaptively adjusts the line parameters in response to changes in R_f , ensuring that $\dot{U}_f \approx 0$ and $\dot{I}_f \approx 0$.

Fig. 2 illustrates the flowchart of the flexible arc

suppression method with adaptive line parameters.

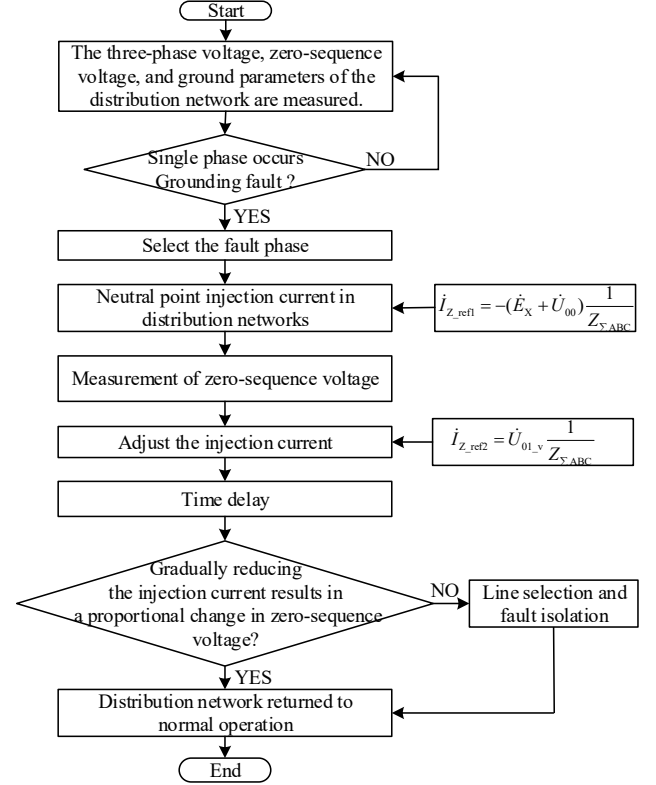


Fig. 2. Flowchart of the flexible arc suppression method with adaptive line parameters.

During normal operation of the distribution network, the ground parameters, bus zero-sequence voltage, and three-phase voltage are continuously measured in real time. Upon the occurrence of a single-phase grounding fault, phase selection must be conducted. Once the fault phase is identified, the reference value \dot{I}_{Z_ref1} for the current control target is calculated according to (25), and current is injected into the neutral point of the distribution network via the FASD. Subsequently, the zero-sequence voltage after the current injection is measured, and the next reference value \dot{I}_{Z_ref2} for the current control target is computed. The current is then injected into the neutral point of the distribution network through the FASD again. After a certain delay, the injection current is gradually reduced. If the fault arc has been extinguished, the zero-sequence voltage will change linearly, according to the homogeneity theorem, indicating a transient single-phase grounding fault. In this case, the distribution network returns to normal operation, and the arc suppression device is disengaged. However, if the zero-sequence voltage changes nonlinearly, it is identified as a permanent single-phase ground fault, prompting the activation of the fault line selection device to isolate the faulted line [10].

IV. SIMULATION AND EXPERIMENTAL VERIFICATION

A. Simulation Parameter Settings

To verify the correctness and effectiveness of the proposed arc suppression method, a distribution network model, as shown in Fig. 3, is established using PSCAD/EMTDC simulation software.

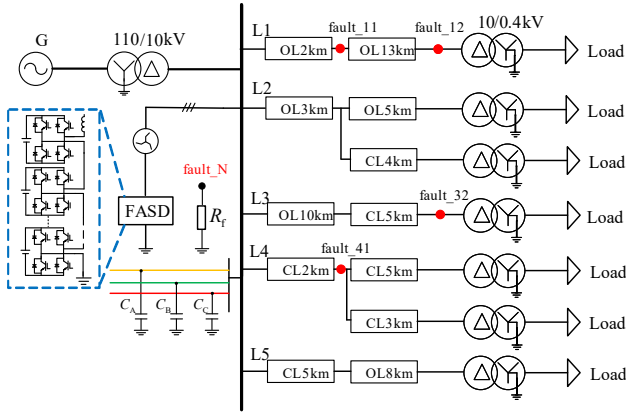


Fig. 3. Schematic diagram of distribution network simulation model.

The parameter settings for the distribution network simulation model are as follows: the power supply voltage is 110 kV; the main transformer is connected in a Y/ Δ configuration with a ratio of 110 kV / 10 kV. A step-down transformer, with a ratio of 10 kV / 0.4 kV, connects the load. The selection of distribution network line parameters is referenced from [29], as shown in Table I.

TABLE I

Line type	Positive-sequence of lines			Zero-sequence of lines		
	R_1 (Ω/km)	L_1 (mH/km)	C_1 ($\mu\text{F}/\text{km}$)	R_0 (Ω/km)	L_0 (mH/km)	C_0 ($\mu\text{F}/\text{km}$)
OL	0.17	1.21	0.011	0.23	5.48	0.008
CL	0.12	0.52	0.29	0.35	1.54	0.26

The distribution network consists of five feeders, with line types including overhead line (OL), cable line (CL), and cable-overhead hybrid lines. To simulate conditions with asymmetric ground parameters, capacitors C_A , C_B , and C_C are connected to the distribution network bus. The asymmetry of the network is 3.5%, and the total capacitance C_0 to ground is 45.18 μF . The simulation parameters are shown in Table II.

TABLE II

SIMULATION PARAMETERS	
Parameters	Value
Line-to-line voltage	10 [kV]
Grid frequency	50 [Hz]
Sample frequency	20 [kHz]
Filter inductance	50 [mH]
Number of H-briges in CHB	12
DC-link voltage of each HB	800 [V]
Proportional coefficient K_p	441
Integral coefficient K_i	1000

In addition, the fault points on the feeder are set at fault_11, fault_12, fault_32, and fault_41 in Fig. 3 to simulate the effect of line impedance voltage drop at various fault positions on the arc suppression method. Under normal operating conditions of the distribution network, the line voltage drop typically does not exceed 10% of the rated voltage, with a maximum allowable voltage drop from the bus to the feeder end of 606V. Consequently, the load current of each feeder in the simulation is configured based on this maximum voltage drop. The transition resistance R_f is set to 10 Ω , 100 Ω , and 1 k Ω . The FASD injects current into the neutral point through a grounding transformer.

B. Simulation Verification

It is assumed that a C-phase grounding fault occurs at 0.04 s in the distribution network, and the FASD is activated at 0.12 s. The reference value for the injection current of the FASD is calculated using (25). At 0.12 s, the injection current reference value of the FASD is set to i_{01_ref} ; after the current is injected, i_{02_ref} is calculated using the proposed flexible arc suppression method with adaptive line parameters. At 0.22 s, the injection current reference value of the FASD is switched to i_{02_ref} . The current waveforms for the single-phase grounding fault under various operating conditions are shown in Fig. 4 to Fig. 7.

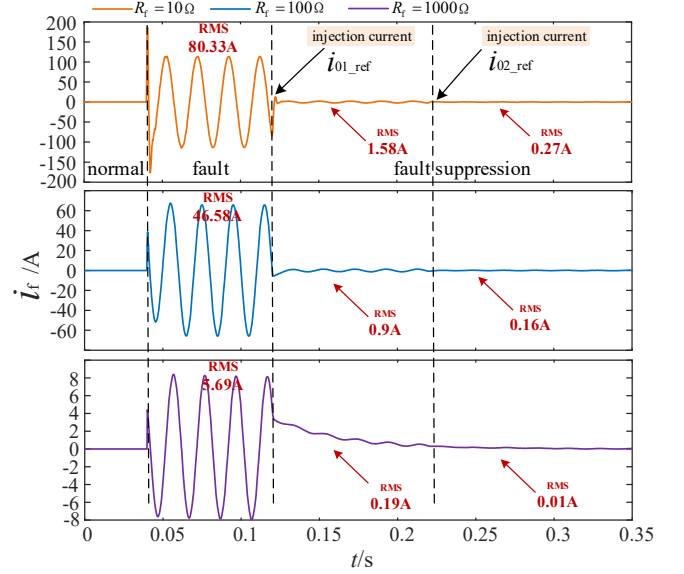


Fig. 4. Single-phase grounding is set at fault_11.

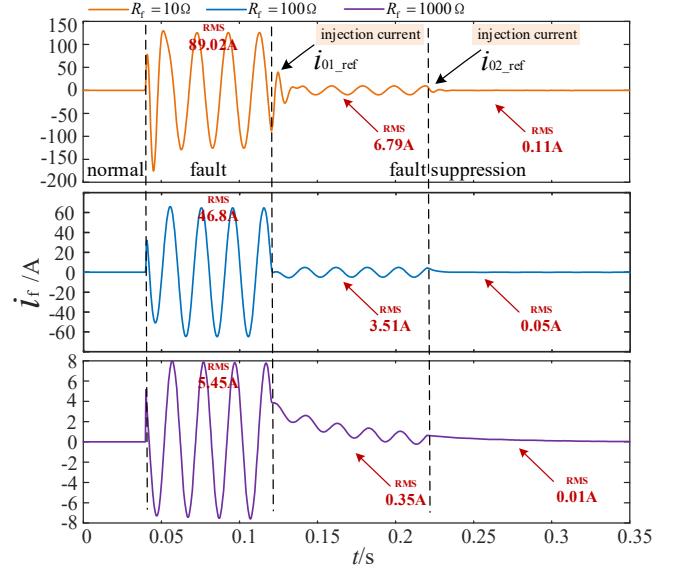


Fig. 5. Single-phase grounding is set at fault_12.

From Fig. 4 and Fig. 5, it can be observed that during the interval from 0.12s to 0.22s, when the injection current reference value of the FASD controller is i_{01_ref} , the fault point current in Fig. 5 is less suppressed compared to Fig. 4. This is because the fault location fault_12 in Fig. 5 is farther from the bus head than the fault location fault_11 in Fig. 4, resulting in a greater line voltage drop. Consequently, when the injection

current reference value of the FASD is i_{01_ref} , a larger line voltage drop leads to a higher residual current after current injection. These simulation results are consistent with the previous analysis. During the interval from 0.22s to 0.35s, when the reference value of the injection current is switched from i_{01_ref} to i_{02_ref} , the suppression of the fault point current in Fig. 5 is comparable to that in Fig. 4, achieving $i_f \approx 0$ A. This demonstrates the effectiveness of the proposed flexible arc suppression method with adaptive line parameters.

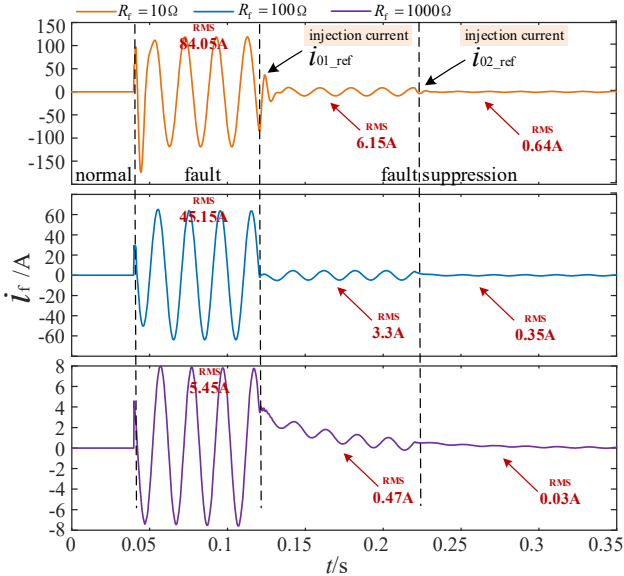


Fig. 6. Single-phase grounding is set at fault_32.

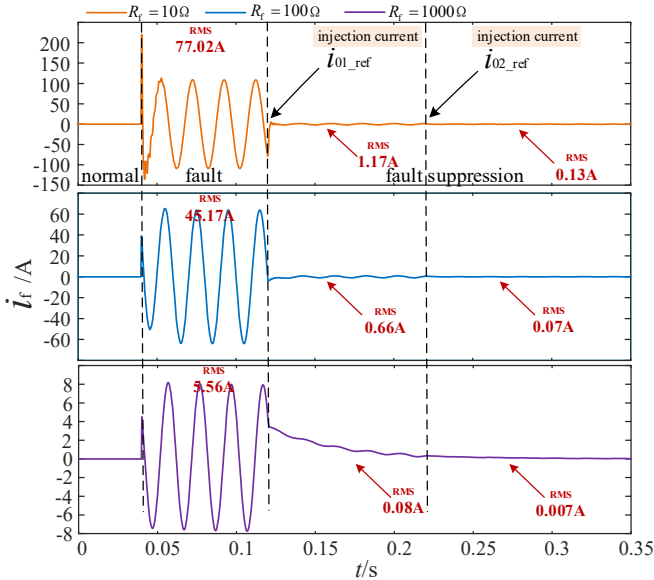


Fig. 7. Single-phase grounding is set at fault_41.

Fig. 6 and Fig. 7 demonstrate that during the time interval from 0.12s to 0.22s, when the FASD controller injection current reference value is i_{01_ref} , the line voltage drop at the fault location fault_32 in Fig. 6 is higher compared to that at the fault location fault_41 in Fig. 7. Consequently, the suppression of the fault point current in Fig. 6 is less effective than in Fig. 7. This discrepancy is attributable to the greater line voltage drop associated with fault_32, which results in a larger residual

current. These observations are consistent with the prior analysis, which indicates that an increased line voltage drop correlates with a higher residual current. During the interval from 0.22 s to 0.35 s, when the reference value of the injection current is switched from i_{01_ref} to i_{02_ref} , the suppression of the fault point current in Fig. 6 achieves a level comparable to that in Fig. 7, effectively reducing $i_f \approx 0$ A. This result underscores the efficacy of the proposed flexible arc suppression method with adaptive line parameters. Furthermore, as illustrated in Fig. 4 through Fig. 7, when $R_f = 1$ k Ω , the fault point current exhibits a transient DC attenuation component, which is influenced by ground capacitance, line inductance, and transition resistance. This attenuation is typically observed over approximately 2 to 3 cycles. The simulation results validate the effectiveness of the proposed method.

From Fig. 4 to Fig. 7, it is observed that single-phase grounding faults occur at fault_11, fault_12, fault_32, and fault_41, as shown in Fig. 3. When the transition resistance R_f is 10 Ω , 100 Ω , and 1k Ω , respectively, the FASD calculates the reference value of the injected current using the proposed flexible arc suppression method, which adapts to variations in line parameters. Once the reference value is applied, the current i_f at the grounding fault point is effectively suppressed to near 0 A. Furthermore, when the FASD controller switches the injection current reference value from i_{01_ref} to i_{02_ref} , i_f is continuously suppressed, further reducing its value.

The simulation results indicate that when the three-phase ground parameters of the distribution network are asymmetric, and the single-phase grounding fault occurs at different locations with varying transition resistance, the proposed flexible arc suppression method effectively adapts to changes in line voltage drop and transition resistance. This method ensures that the fault current $i_f \approx 0$ A.

C. Physical Experimental Verification

To further validate the effectiveness of the flexible arc suppression method for adaptive line parameter variations proposed in this paper, a physical simulation system platform for the distribution network and a physical prototype of the FASD were constructed, as illustrated in Fig. 8.

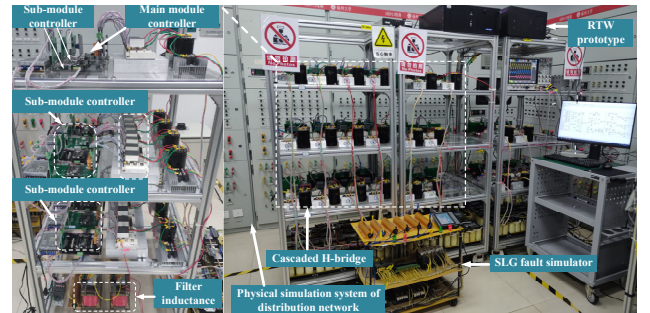


Fig. 8. Physical experiment platform for distribution network and prototype of FASD

In Fig.8, the physical simulation system for the distribution network was constructed using the similarity principle, with a 380V physical system modeling a 10kV distribution network. The platform comprises a distribution network physical simulation system, a single-phase grounding fault device, and a cascaded H-bridge flexible arc suppression prototype. The

distribution network simulation system and the single-phase grounding fault device are capable of simulating single-phase grounding faults for both overhead and cable lines. Fault currents are suppressed by the cascaded H-bridge flexible arc suppression prototype. The control system of the cascaded H-bridge prototype consists of a main module controller and sub-module controllers. The hardware system of the single-phase FASD consists of a main module and sub-modules. Each sub-module includes an H-bridge unit and its corresponding controller, which is responsible for controlling and protecting the H-bridge unit. The main module communicates with and controls the sub-modules.

To verify the effectiveness of the proposed method, transition resistances of $R_f = 10\ \Omega$, $100\ \Omega$, and $1\text{k}\Omega$ were tested, with the total capacitance to ground $C_{\Sigma ABC} = 48.84\ \mu\text{F}$. In addition, to simulate asymmetrical ground parameters, capacitors C_A , C_B , and C_C were added to the bus of the physical simulation platform for the distribution network, as shown in Fig. 8. Among them, $C_A = 0\ \mu\text{F}$, $C_B = 1\ \mu\text{F}$, and $C_C = 4.7\ \mu\text{F}$. The FASD controller utilizes proportional-integral (PI) control. The experimental parameters are shown in Table III.

TABLE III
EXPERIMENTAL PARAMETERS

Parameters	Value
Line-to-line voltage	380 [V]
Grid frequency	50 [Hz]
Sample frequency	10 [kHz]
Switching frequency	5 [kHz]
Filter inductance	50 [mH]
Number of H-bridges in CHB	6
DC-link voltage of each HB	60 [V]
Proportional coefficient K_p	150
Integral coefficient K_i	0.1

It is assumed that a single-phase (Phase A) grounding fault occurs at 0.1s, with FASD being activated at 0.16s. The grounding suppression waveforms under various grounding fault conditions are presented in Fig. 9 and Fig. 10.

In these figures, u_H represents the output voltage of the FASD, u_N denotes the system neutral point voltage, i_{in} is the current injected by the FASD, and i_f is the single-phase ground fault current. i_{01_ref} and i_{02_ref} represent the injection current reference values for the FASD at different time intervals. These reference values are determined using (25).

Fig. 9 shows that the FASD effectively suppresses ground fault current, even with variations in R_f , when the distribution network maintains symmetry in ground parameters. Fig. 9 shows that when the control target value i_{01_ref} of the FASD controller is switched to i_{02_ref} , the transition occurs smoothly and effectively suppresses the ground fault current i_f . Additionally, the suppression of fault current following the switch from i_{01_ref} to i_{02_ref} is more effective compared to the suppression before the switch. When R_f varies from $10\ \Omega$ to $1\ \text{k}\Omega$, i_{02_ref} provides more effective fault current suppression compared to i_{01_ref} . As R_f increases, the difference in fault current suppression between i_{01_ref} and i_{02_ref} gradually diminishes, approaching equivalence.

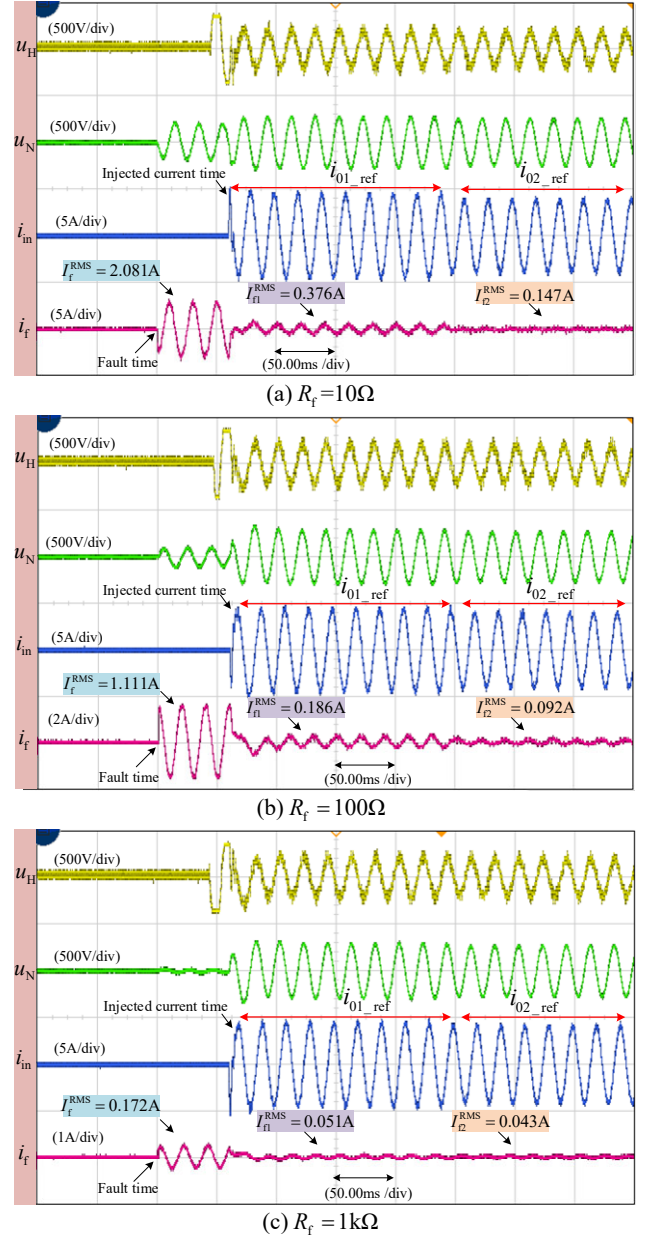


Fig. 9. Single-phase ground fault waveform for symmetrical ground parameters. (a) $R_f = 10\ \Omega$. (b) $R_f = 100\ \Omega$. (c) $R_f = 1\ \text{k}\Omega$.

Fig. 10 shows that when the control target value i_{01_ref} of the FASD is switched to i_{02_ref} under conditions of asymmetrical distribution network parameters to ground, the transition occurs smoothly, effectively suppressing the ground fault current i_f . Additionally, the fault current suppression after switching to i_{02_ref} is more effective than before the switch. Additionally, the ground fault current suppression waveform in Fig. 10 is consistent with that in Fig. 9 and will not be reiterated here. The experimental results demonstrate that the proposed flexible arc suppression method, which adapts to line parameter variations, effectively suppresses ground fault current even under the influence of line voltage drop and asymmetry in ground parameters. Compared to traditional methods, the proposed approach exhibits a significantly improved fault current suppression performance.

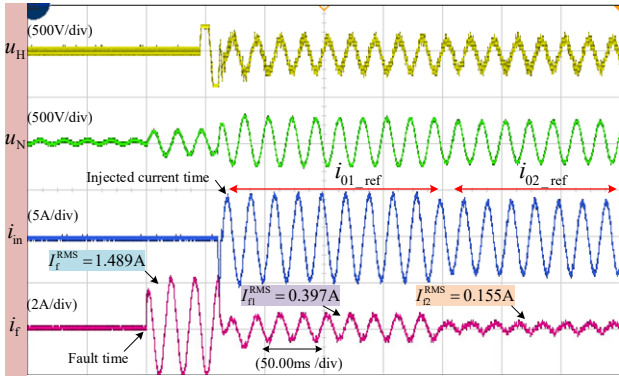
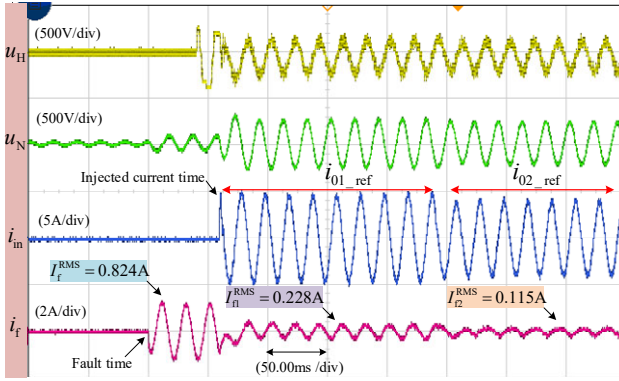
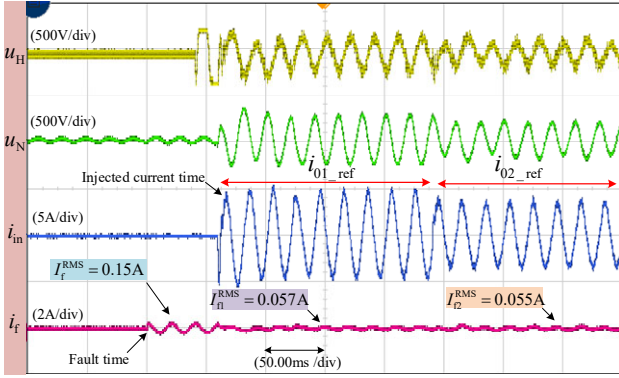
(a) $R_f = 10\Omega$ (b) $R_f = 100\Omega$ (c) $R_f = 1k\Omega$

Fig. 10. Single-phase ground fault waveform for asymmetrical ground parameters. (a) $R_f = 10\Omega$. (b) $R_f = 100\Omega$. (c) $R_f = 1k\Omega$.

This study compares the proposed method with other arc suppression methods using an existing physical experimental platform, with results shown in Tables IV and V.

In Tables IV and V, Method 1 is a voltage-type flexible arc suppression method, as presented in [10], and [14], while Method 2 is a current-type flexible arc suppression method, as presented in [20], and [26].

Additionally, L_1 and L_2 in the table represent different fault locations. Compared to L_1, L_2 is farther from the bus head. R_f denotes the transition resistance at the fault point. I_f^{RMS} refers to the effective value of the fault current. I_{f1}^{RMS} represents the effective value of the fault current after the FASD is activated. η indicates the percentage of fault current suppression, $\eta = \frac{I_f^{RMS} - I_{f1}^{RMS}}{I_f^{RMS}} \times 100\%$.

Fault point	Fault conditions		Method 1	Method 2	This article
	R_f / Ω	I_f^{RMS} / A	I_{f1}^{RMS} / A	I_{f1}^{RMS} / A	I_{f1}^{RMS} / A
L_1	10	2.81	0.476	0.375	0.283
	100	1.448	0.256	0.197	0.149
	1000	0.198	0.031	0.028	0.028
L_2	10	2.081	0.713	0.376	0.147
	100	1.111	0.306	0.186	0.092
	1000	0.172	0.048	0.051	0.043

Fault point	Fault conditions		Method 1	Method 2	This article
	R_f / Ω	I_f^{RMS} / A	$\eta / \%$	$\eta / \%$	$\eta / \%$
L_1	10	2.81	83.1	86.7	89.9
	100	1.448	82.3	86.4	89.7
	1000	0.198	84.3	85.9	85.9
L_2	10	2.081	65.7	81.9	92.9
	100	1.111	72.5	83.3	91.7
	1000	0.172	72.1	70.4	75

From Tables IV and V, it can be observed that when the single-phase grounding fault occurs at L_1 with R_f values of 10Ω and 100Ω , the fault current suppression percentage η of the proposed method is slightly higher than that of Methods 1 and 2. The η of Method 2 is slightly higher than that of Method 1. As R_f increases, the η values for all three arc suppression methods converge. Similarly, when the single-phase grounding fault occurs at L_2 with R_f values of 10Ω and 100Ω , the η of the proposed method is higher than that of Methods 1 and 2. The η of Method 2 is higher than that of Method 1. As R_f increases, the η values for all three methods tend to become similar. Furthermore, under different R_f conditions, the η values for Methods 1 and 2 at L_2 are lower than those at L_1. The η of Method 1 is most significantly affected by the fault location at L_2.

It can be observed that, under low resistance conditions, Methods 1 and 2 are significantly affected by line voltage drop, especially Method 1. Under high resistance conditions, Methods 1 and 2 can neglect the influence of line voltage drop. The method proposed in this article demonstrates strong fault suppression capability, regardless of whether the resistance is low or high.

In summary, the flexible arc suppression method proposed in this article is unaffected by line voltage drop, enabling more effective suppression of ground fault current and achieving the goal of zero residual current. Furthermore, the proposed method ensures reliable arc suppression under various operating conditions.

V. CONCLUSION

The traditional current-type flexible arc suppression method is significantly influenced by grounding fault parameters, which limits its effectiveness in achieving zero residual current suppression for ground faults, thereby compromising reliable arc suppression. To address this limitation, a flexible arc suppression method with adaptive line parameter variations is proposed to enhance performance and reliability.

After the FASD injects current based on the specified

reference value, the effectiveness of zero-sequence voltage regulation by the injected current directly affects the magnitude of the residual ground fault current. Based on the characteristics of both the newly derived and original injection current algorithms for zero-sequence voltage regulation and ground fault suppression, this paper proposes an adaptive injection current arc suppression algorithm that adjusts to changes in line parameters. The proposed algorithm does not require measurements of fault location, line impedance, and load current. Compared to traditional injection current arc suppression algorithms, the proposed method demonstrates enhanced adaptability to variations in grounding fault parameters and achieves superior performance in ground fault current suppression.

REFERENCES

- [1] X. X. Wei, D. C. Yang, X. W. Wang, B. Wang, and J. Gao, "Faulty Feeder Detection Based on Fundamental Component Shift and Multiple-Transient-Feature Fusion in Distribution Networks," *IEEE Trans. Smart Grid*, vol. 12, no. 2, pp. 1699-1711, Mar. 2021.
- [2] Y. C. Hou, Q. Guo, C. M. Tu, F. Xiao, L. Wang, F. Jiang, K. Yu, and X. Wang, "A review of single-phase-to-ground fault regulation devices for distribution networks," *Renew. Sustain. Energy Rev.*, vol. 200, Aug. 2024, Art. no. 114602.
- [3] W. S. P. Fernando, M. A. Mahmud, S. N. Islam, M. A. Barik, and N. Hosseinzadeh, "A comprehensive review of control techniques for compensating the fault current in resonant grounded distribution networks: From the perspective of mitigating powerline bushfires," *IET Gener. Trans. Distrib.*, Vol. 17, no. 1, pp. 1-16, Jan. 2023.
- [4] J. R. Tang, Y. Li, C. Q. Yuan, and Y. C. Qiu, "Faulted Feeder Identification Based on Active Adjustment of Arc Suppression Coil and Similarity Measure of Zero-Sequence Currents," *IEEE Trans. Power Del.*, vol. 36, no. 6, pp. 3903-3913, Dec. 2021.
- [5] F. Rong, C. H. Huang, H. W. Liu, and C. Liu, "A Novel Topology for Grounding Fault Voltage Compensation Based on Voltage Clamping," *IEEE Sensors J.*, 2023, 17(1): 579-588. vol. 17, no. 1, pp. 579-588, Mar. 2023.
- [6] P. Wang, B. C. Chen, C. H. Tian, B. Sun, M. Zhou, and J. X. Yuan, "A Novel Neutral Electromagnetic Hybrid Flexible Grounding Method in Distribution Networks," *IEEE Trans. Power Del.*, vol. 32, no. 3, pp. 1350-1358, Jun. 2017.
- [7] M. Mitolo, R. Musca, M. Tartaglia, and G. Zizzo, "Electrical Safety Analysis in the Presence of Resonant Grounding Neutral," *IEEE Trans. on Ind. Applicat.*, 2019, 55(5): 4483-4489. vol. 55, no. 5 pp. 4483-4489, Oct. 2019.
- [8] M. F. Guo, X. D. Zeng, D. Y. Chen, and N. C. Yang, "Deep-Learning-Based Earth Fault Detection Using Continuous Wavelet Transform and Convolutional Neural Network in Resonant Grounding Distribution Systems," *IEEE Sensors J.*, vol. 18, no. 3 pp. 1291-1300, Feb. 2018.
- [9] Z. J. Huang, Q. Guo, C. M. Tu, Y. C. Hou, F. Jiang, X. Wang, F. Xiao, and Z. K. Xiao, "A Non-neutral alternate arc suppression method for single phase grounding fault in active distribution network," *Int. J. Elect. Power Energy Syst.*, vol. 152, no. 3, Oct. 2023, Art. no. 109182
- [10] W. Wang, X. J. Zeng, L. J. Yan, X. Y. Xu, and J. M. Guerrero, "Principle and Control Design of Active Ground-Fault Arc Suppression Device for Full Compensation of Ground Current," *IEEE Trans. Ind Electron.*, Vol. 64, no. 6, pp. 4561-4570, Jun. 2017.
- [11] M. Roser, G. Stumberger, "Improving the power supply reliability in resonant earthed systems by fault current path control established through Faulted Phase earthing Switch," *Int. J. Elect. Power Energy Syst.*, vol. 64, pp. 714-722, Jan. 2015.
- [12] K. L. Liu, S. Zhang, B. R. Li, C. Zhang, B. Y. Liu, H. Jin, and J. F. Zhao, "Flexible Grounding System for Single-Phase to Ground Faults in Distribution Networks: A Systematic Review of Developments," *IEEE Trans. Power Del.*, vol. 37, no. 3, pp. 1640-1649, Jun. 2022.
- [13] B. S. Fan, G. Z. Yao, W. Wang, X. J. Zeng, J. M. Guerrero, K. Yu, and C. Zhuo, Principle and Control Design of a Novel Hybrid Arc Suppression Device in Distribution Networks[J]. *IEEE Trans. Ind. Electron.*, Vol. 69, no. 1, pp. 41-51, Jan. 2022.
- [14] X. M. Luan, X. P. Li, S. Y. Wu, C. J. Jia, H. K. Mei, and L. X. Gao, "Arc Suppression Control with Adaptive Parameters of Active Grounding Device Considering Ground Fault Resistance Uncertainty," *IEEE Trans. Power Del.*, vol. 39, no. 1, pp. 426-435, Feb. 2024.
- [15] L. Li, X. J. Zeng, H. Bai, K. Yu, J. Z. Li, H. H. Peng, Z. Wang, H. J. Luo, and F. H. Wang, "Analysis and design of flexible arc suppression device based on proportional series lagging control," *Int. J. Elect. Power Energy Syst.*, vol. 143, Dec. 2022, Art. no. 108478.
- [16] B. L. Zhang, M. F. Guo, Z. Y. Zheng, and Q. T. Hong, "Fault Current Limitation With Energy Recovery Based on Power Electronics in Hybrid AC-DC Active Distribution Networks," *IEEE Trans. Power Electron.*, vol. 38, no. 10, pp. 12593-12606, Oct. 2023.
- [17] Z. Y. Zheng, M. F. Guo, T. Jin, and J. H. Liu, "A novel method of insulation parameters measurement based on hybrid flexible arc suppression device in distribution networks," *Int. J. Elect. Power Energy Syst.*, vol. 130, Sep. 2021, Art. no. 106982.
- [18] K. Y. Chen, W. H. Zhang, and X. Y. Xiao, "Faulted terminal open circuit voltage controller for arc suppression in distribution network," *IET Gener. Trans. Distrib.*, Vol. 14, no. 14, pp. 2763-2770, Sep. 2020.
- [19] Y. C. Hou, Q. Guo, C. M. Tu, F. Jiang, L. Wang, X. Wang, and F. Xiao, "Adaptive Active Voltage-Type Arc Suppression Strategy Considering the Influence of Line Parameters in Active Distribution Network," *IEEE Trans. Ind Electron.*, Vol. 70, no. 5, pp. 4799-4808, May. 2023.
- [20] Y. M. Chen, S. Lu, X. D. Zhou, and S. B. Liang, "Two-Phase Current Injection Method for Single Line-to-Ground Fault Arc-Suppression With Revised STATCOM," *IEEE Access*, vol. 8, pp. 188299-188308, Oct. 2020.
- [21] M. F. Guo, Y. H. Jiao, Z. Y. Zheng, J. H. Lin, and Q. T. Hong, "Online Split-phase Identification of Asymmetric Parameters Between Distribution Lines and Ground for Unbalanced Voltage Compensation Based on Power Electronics," *IEEE Trans. Power Electron.*, vol. 39, no. 8, pp. 1-12, Aug. 2024.
- [22] J. Z. You, M. F. Guo, Z. Y. Zheng, and X. B. Liu, "Flexible composite suppression method for ground arc in resonant grounding system," *High Voltage*, vol. 8, no. 6, pp. 1296-1305, Dec. 2023.
- [23] M. Barzegar-Kalashani, M. A. Mahmud, M. A. Barik, and A. M. T. Oo, "Control of arc suppression devices in compensated power distribution systems using an integral sliding mode controller for mitigating powerline bushfires," *Int. J. Elect. Power Energy Syst.*, vol. 134, Jan. 2022, Art. no. 107481.
- [24] K. Yu, S. Q. Liu, X. J. Zeng, H. H. Peng, F. Liu, and Z. Wang, "A Novel Insulation Parameter Online Measuring Technique Based on Two Voltage Transformers for Distribution Networks," *IEEE Trans. Power Del.*, vol. 36, no. 6, pp. 3383-3392, Dec. 2021.
- [25] K. Yu, J. K. Li, X. J. Zeng, H. H. Peng, Y. R. Ni, F. Liu, and C. Zhuo, "Insulation Parameter Online Measurement Technology Based on Extended Zero-Sequence Circuits for Resonant Grounding Distribution Networks," *IEEE Trans. Power Del.*, vol. 37, no. 6, pp. 4679-4689, Dec. 2022.
- [26] Z. Y. Zheng, H. Y. Qiu, B. L. Zhang, M. F. Guo, S. Y. Lin, and W. Q. Cai, "A novel flexible fault eliminator with active disturbance rejection and soft grid-connection in distribution networks," *Int. J. Elect. Power Energy Syst.*, vol. 154, Dec. 2023, Art. no. 109425.
- [27] W. S. P. Fernando, M. A. Mahmud, "A Nonlinear Discrete-Time Backstepping Model Predictive Controller Design for Active Arc Suppression Coils in Compensated Power Systems to Mitigate Powerline Bushfire Hazards," *IEEE Trans. Ind Electron.*, Vol. 71, no. 11, pp. 15077-15088, Nov. 2024.
- [28] B. L. Zhang, M. F. Guo, M. Lak, C. M. Lin, and Q. T. Hong, "Minimizing Required DC Sources of Cascaded H-Bridge Multilevel Converter for Fault Suppression in Active Distribution Networks," *IEEE Trans. Ind Electron.*, early access, Nov. 2024. doi: 10.1109/TIE.2024.3488279
- [29] J. H. Lin, M. F. Guo, Q. T. Hong, and R. Jiang, "An Earth Fault Diagnosis Method Based on Online Dynamically Calculated Thresholds for Resonant Ground Systems," *IEEE Trans. Smart Grid*, vol. 15, no. 4, pp. 3459-3473, Jul. 2024.



fault in distribution networks.

Guojun Zhao received the B.S. and M.S. degrees in electrical engineering from Hubeiminzu University, Enshi, China, in 2018, 2023. He is currently working toward the Ph.D. degree in electrical engineering with the Fuzhou University, Fujian, China. His research interests include the protection control, and flexible arc suppression of single-line-to-ground



protection and control in future networks with high penetration of renewables. Dr. Hong is a member of IEEE Working Group P2004 and IEEE Task Force on Cloud-Based Control and Co-Simulation of Multi-Party Resources in Energy Internet. He was a Regular Member of the completed CIGRE WG B5.50.

Qiteng Hong (Senior Member, IEEE) received the B.Eng. (Hons.) and Ph.D. degrees in electronic and electrical engineering from the University of Strathclyde, Glasgow, U.K., in 2011 and 2015, respectively. He is currently a Senior Lecturer (Associate Professor) with the University of Strathclyde. His current research focuses on power system



Engineering and Automation. He is currently an Professor with the Fuzhou University, Fuzhou, China. His research interests include the information processing, protection control, and flexible arc suppression of single-line-to-ground fault in distribution networks.

Moufa Guo (Member, IEEE) received the B.S. and M.S. degrees in electrical engineering from the Fuzhou University, Fuzhou, China, in 1996 and 1999, respectively, and the Ph.D. degree in electrical engineering from the Yuan Ze University, Taoyuan, Taiwan, in 2018. Since 2000, he has been with the Fuzhou University, where he is currently a



research interest is the protection and control of power systems with a high penetration of renewable energy resources with power electronics.

Binlong Zhang (Student Member, IEEE) received his B.S. degree in electrical engineering from Fuzhou University, Fuzhou, China, in 2020. He is currently working toward a Ph.D. degree in electrical engineering at Fuzhou University, Fuzhou, China, and toward another Ph.D. degree in electrical engineering at Yuan Ze University, Taoyuan, Taiwan. His main



research interests include power distribution system automation, flexible active arc suppression of single-phase ground fault, protection, and control of distribution systems.

Zeyin Zheng (Member, IEEE) received the B.S. degree in electrical engineering from the Fuzhou University, Fuzhou, China, in 2014, and the Ph.D. degree in electrical engineering from the Fuzhou University and the Yuan Ze University, Taoyuan, Taiwan, in 2021. He is currently an Associate Professor with the Fuzhou University, Fuzhou, China. His